IEEE Access
Multidisciplinary | Rapid Review | Open Access Journal

Received July 4, 2021, accepted August 6, 2021, date of publication August 9, 2021, date of current version August 16, 2021.

Digital Object Identifier 10.1109/ACCESS.2021.3103944

NOMA-Based Integrated Satellite Terrestrial Networks With Relay Selection and Imperfect SIC

HAIFENG SHUAI[1], KEFENG GUO[1], KANG AN[2], AND SHIBING ZHU[1]
[1]School of Space Information, Space Engineering University, Beijing 101416, China
[2]Sixty-Third Research Institute, National University of Defense Technology, Nanjing 210007, China

Corresponding author: Kefeng Guo (guokefeng.cool@163.com)

This work was supported in part by the National Science Foundation of China under Grant 61901502 and Grant 62001517, in part by the National Postdoctoral Program for Innovative Talents under Grant BX20200101, in part by the Research Project of Science and Technology on Complex Electronic System Simulation Laboratory under Grant DXZT-JC-ZZ-2019-005, and in part by the Research Project of Space Engineering University under Grant 2020XXAQ01.

ABSTRACT Integrated satellite terrestrial networks (ISTNs) are becoming a hot research topic in recent years due to the capabilities of high quality, high throughput, and seamless coverage. However, the limited spectrum resources are difficult to meet the needs of a large number of users in ISTNs, and the obstacles and shadowing will seriously affect the communication quality of networks. In this regard, cooperative transmission of non-orthogonal multiple access (NOMA)-assisted ISTNs with the help of multiple terrestrial relays are established to enhance the spectrum efficiency and enlarge the transmission coverage. In this paper, we investigate the performance of NOMA-based ISTNs with relay selection and imperfect successive interference cancellation (SIC). Particularly, the partial relay selection (PRS) scheme is used in the considered system to reach the balance of system performance and complexity. Owing to practical constraints, the imperfect SIC is analyzed for the networks. Based on the PRS scheme and imperfect SIC, we obtain the closed-form expressions for the outage probability (OP) and ergodic capacity (EC) of the considered networks. Besides, to get further insights of key system parameters, the asymptotic analysis for the OP is also derived. Finally, numerical and simulation results are presented to validate the correctness of our analytical results.

INDEX TERMS Integrated satellite terrestrial networks (ISTNs), non-orthogonal multiple access (NOMA), relay selection, successive interference cancellation (SIC).

I. INTRODUCTION

Recent years, satellite communication (SatCom) has been the key part of fifth-generation (5G) networks and beyond 5G (B5G) networks due to its inherent characteristics such as high throughput, wide coverage, high reliability, and disregarding geographic boundaries for propagation, which will be an excellent complement to the current terrestrial communications [1]–[4]. Therefore, incorporating SatCom into existing terrestrial communication systems has become mainstream research today, which is the basic architecture of integrated satellite terrestrial networks (ISTNs) [5]–[7]. However, due to the obstacles and shadowing between the satellite and terrestrial users, the transmission quality of the direct link of the ISTNs is low or even interrupted [8]–[10]. In this regard, integrated satellite terrestrial relay networks (ISTRNs) are established to overcome this problem, which can utilize the terrestrial relay stations to receive and forward satellite signals to terrestrial users [11], [12].

Increasing the utilization of the spectrum is the requirement for the B5G networks. However, the traditional orthogonal multiple access (OMA) cannot meet the requirements of spectrum utilization efficiency [13]. The emergence of non-orthogonal multiple access (NOMA) scheme can overcome this shortcoming, which can transmit the wireless signals to multiple users at the same time/frequency through power/code domain multiples [14]–[16]. Furthermore, NOMA scheme is recognized as one of the vital core technologies for massive user access and ultra-high capacity requirements in the future wireless communication networks.

A. RELATED WORKS

The ISTRNs have become a popular research direction in recent years. Besides, it is recognized as a Digital

The associate editor coordinating the review of this manuscript and approving it for publication was Jenny Mahoney.

Video-Broadcast (DVB) standard for service between Satellites and Handheld devices (SH) in the frequency band below 3GHz [8], [17], [19], [20]. In [17], the performance of OP and ergodic capacity (EC) was analyzed for the ISTRNs with decode-and-forward (DF) protocol, where two multiuser scheduling schemes were considered to improve transmission performance. In [18], the authors introduced the cognitive radio technology to ISTRNs, which can improve the performance of outage probability (OP) of the considered system. The authors of [19] chose an unmanned aerial vehicle (UAV) instead of the terrestrial relay, specifically, the energy efficiency (EE) was enhanced through beamforming (BF) scheme. In [20], the authors investigated the NOMA-based ISTRNs with DF protocol under spectrum sharing environment, which can enhance the spectrum efficiency of the system.

Due to the wide coverage of the satellite beam, one satellite beam often covers many terrestrial users, thus multiple relays scenario in the ISTRNs is a common scene [21], [22]. To obtain the balance between the system performance and system complexity, relay selection scheme is often considered in the multiple terrestrial relay networks [23]–[29]. In [23]–[25], two-stage relay selection schemes were considered in cooperative NOMA-based terrestrial wireless communication systems, where relays were working in full-duplex (FD) or half-duplex (HD) mode with amplify-and-forward (AF) or DF protocol, and the system can get superior outage behaviors. In [26], the authors employed a max-max relay selection strategy for the ISTRNs with AF protocol, which permitted a reduction in the OP of the considered system. Partial and opportunistic relay selection (ORS) schemes were analyzed for satellite-terrestrial spectrum sharing system in [27], which enhanced the performance of system OP. In [28], the authors introduced wireless content caching to satellite-terrestrial relay networks, and an optimal relay selection policy was adopted to improve spectral efficiency and outage performance. The authors of [29] proposed a Vickrey auction-based secondary relay selection strategy in ISTRNs, both the DF and AF protocols were considered, and the total capacity of the system was increased.

As mentioned before, the limited spectrum resources in the ISTRNs needs to be enhanced with high efficiency. Hence, owing to the inherent characters, the NOMA scheme has been used widely in the ISTRNs to improve the spectrum efficiency [30]–[38]. In [31]–[33], the authors introduced the NOMA and cooperative NOMA schemes into the ISTRNs, especially, the performance of OP and EC were obtained to validate the superiority of the proposed framework. The authors of [34] investigated the performance of the NOMA-based integrated satellite-terrestrial networks with cooperative device-to-device (D2D) scheme, and achieved significant sum rate and spectral efficiency gains. In [35], the authors derived the closed-form expression of OP for a cooperative NOMA-based ISTRN where the user with better channel conditions was regarded as a DF relay to assist the user with worse channel conditions. The authors of [36] integrated NOMA scheme and wireless content delivery into SatCom networks, specifically, the expressions of OP and hit probability were derived respectively. In [37], the authors proposed a joint optimization design of NOMA-based ISTRNs where the sum rate of the considered system was improved under satisfying transmission power limitation and quality of service (QoS) requirements. Optimization problem of NOMA-based ISTRNs was analyzed in [38] by considering the effect of perfect and imperfect channel state information (CSI) where the robust beamforming scheme was derived to evaluate the benefit of the NOMA scheme.

In the NOMA scheme, the receivers use SIC technology to decode the received signal. However, for some practical reasons such as synchronization mistakes, error propagation between transmission links, and limitations of receivers performance, it is tough to acquire perfect SIC technology in the receivers. In this condition, imperfect SIC has been taken into account in much recent literature [39]–[43]. In [39], [40], the authors unveiled the significance of SIC in NOMA systems, and systematically analyzed the foundation, requirements and development prospects of SIC technology. In [41], the authors established a two-way relay NOMA system with DF protocol, recalling imperfect SIC and perfect SIC, the analytical expressions of OP and EC were derived. The authors of [42] derived the closed-form expressions of OP and ergodic sum rate (ESR) for a FD cooperative NOMA relay system with imperfect SIC, and compared the performance with the OMA scheme. At present, only a small amount of literature has analyzed the application of imperfect SIC in the NOMA-based SatCom networks [44]–[46]. The authors of [44] researched the outage performance of the imperfect SIC in a NOMA-based hybrid satellite-terrestrial relay network. In [45], [46], the authors introduced an independent residual interference parameter to represent imperfect SIC in the NOMA-based SatCom networks.

B. MOTIVATIONS AND CONTRIBUTIONS

From the above analysis, we know the investigation for the ISTRNs with NOMA scheme has been an active research topic, however, the analysis for the NOMA-based ISTNs with multiple terrestrial relays and imperfect SIC remains unreported, which motivates the construction of this paper.

Particularly, the detailed contributions of this paper can be summarized as follows:

1) We establish a general model for the NOMA-based ISTNs with multiple terrestrial relays and imperfect SIC. A partial relay selection (PRS) scheme is employed to improve the spectrum efficiency. Imperfect SIC is considered due to limitations of receiver performance.
2) In order to obtain the effects of multiple terrestrial relays and imperfect SIC, the closed-form expressions for the OP and EC are derived. The asymptotic analysis is further obtained in high signal-to-noise ratio (SNR) regime to get deeper insights.

3) Finally, Monte Carlo (MC) simulation results validate the correctness of our theoretical results. Furthermore, the impacts of critical parameters on the system performance, including the number of relays, imperfect SIC coefficient, and power allocation coefficients of NOMA, are revealed by simulations.

The rest of this paper is arranged as follows. In Section II, the system model and problem formulation are given. Then, the end-to-end signal-to-interference-plus-noise ratio (SINR) of the system, the optimal relay selection scheme and the statistical property of the channel are presented in Section III. In Section IV, the closed-form and asymptotic expressions of OP are derived. The detailed analysis for the EC is given in Section V. In Section VI, MC simulations are provided to verify the accurateness of our analytical derivation. Finally, the whole article is summarized in Section VII.

Notations: $|\cdot|$ represents the absolute value of a complex scalar. $E(\cdot)$ denotes the expectation operator. $\mathcal{CN}(\mu, \nu)$ is the addictive white Gaussian noise (AWGN) with mean μ and variance matrix ν. $J_i(\cdot)$ indicates the first-kind bessel function of order i. ${}_1F_1(a; b; z)$ stands for the confluent hypergeometric function [42, Eqs. 9.210.1]. $(a)_n = a(a+1)+\ldots+(a+n-1) = \Gamma(a+n)/\Gamma(a)$ represents the Pochhammer symbol [47]. $\Gamma(\cdot)$ denotes the complete gamma function. $diag(\cdot)$ denotes the diagonal matrix. $G_{p,q}^{m,n}(\cdot|\cdot)$ denotes Meijer-G function [42, Eqs. 9.301].

II. SYSTEM MODEL

In this paper, we consider the NOMA-based ISTNs with multiple terrestrial relays which is illustrated in Fig.1, where a satellite source S[1] communicates with two terrestrial users $U_i, i \in \{p, q\}$ adopting the NOMA scheme[2] with the help of a selected relay R_{n^*} ($n \in \{1, 2, \ldots, K\}$) out of K terrestrial relays. We assume that one satellite beam covers multiple terrestrial relays, and S cannot communicate with U_i in the direct link for the reason of blocking caused by occlusions and space path loss caused by extreme weather such as rain and fog.[3] Hence, K terrestrial relays based on half-duplex DF-based spectral sharing protocol are used for collaborative transmission.

The overall transmission can be divided into two time slots. In the first time slot, a superimposed signal is transmitted by satellite S to terrestrial relays which can be expressed as $s = \sqrt{a_p}x_p + \sqrt{a_q}x_q$, where a_i is the power allocation coefficients in NOMA scheme with $a_p + a_q = 1$, and x_i is the target received signal of the terrestrial users U_i obeying

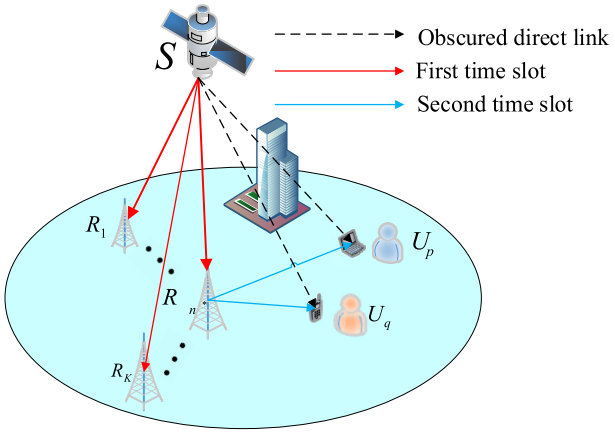

FIGURE 1. System model.

$E(|x_i|^2) = 1$. In this paper, we assume that the channel condition of U_p is inferior to that of U_q so that more power is allocated to U_p, i.e. $a_p > a_q$ [16], [29]. Therefore, the signal received by R_n can be represented as

$$y_R = h_{SR_n}\left(\sqrt{P_S a_p}x_p + \sqrt{P_S a_q}x_q\right) + w_{SR_n}, \tag{1}$$

where P_S is the transmission power of S, w_{SR_n} is the AWGN between S and R_n modeled as $w_{SR_n} \sim \mathcal{CN}\left(0, \sigma_{SR_n}^2\right)$, h_{SR_n} is the channel coefficient of satellite to terrestrial link undergos the shadowed-Rician (SR) fading [48], which is uniformly given by

$$h_{SR_n} = \mathcal{F}_{SR_n} g_{SR_n}, \tag{2}$$

where g_{SR_n} is the SR fading channel complex coefficient. $\mathcal{F}_{SR_n}$ represents a scaling parameter including many actual impact factors, such as antenna gain and free space loss (FSL), which can be written as

$$\mathcal{F}_{SR_n} = \frac{\vartheta\sqrt{\mathcal{G}_{S,SR_n}\mathcal{G}_{R_n,SR_n}}}{f\mathcal{D}_{SR_n}\sqrt{K_B T B}}, \tag{3}$$

where $\vartheta = c/4\pi$, c is the speed of light, f and B represent carrier frequency and bandwidth, respectively. D_{SR_n} denotes the distance of satellite and terrestrial users, K_B is the Boltzmann constant which is always equal to $1.380649 \times 10^{-23} J/K$, and T is the noise temperature of terrestrial receiver. In addition, $\mathcal{G}_{S,SR_n}$ and $\mathcal{G}_{R_n,SR_n}$ denote the satellite beam gain and receive antenna gain, respectively. $\mathcal{G}_{S,SR_n}$ can be conventionally written as

$$\mathcal{G}_{S,SR_n} = \mathcal{G}_{\max}\left(\frac{J_1(\omega)}{2\omega} + 36\frac{J_3(\omega)}{\omega^3}\right)^2, \tag{4}$$

where $\mathcal{G}_{\max}$ denotes the maximal beam gain, J_1 and J_3 represent the first-kind bessel function of order 1 and 3, respectively. $\omega = 2.07123\frac{\sin\varphi}{\sin\varphi_{3dB}}$, where φ is the angle between the terrestrial receiver and the satellite beam, φ_{3dB} denotes the 3-dB angle.

In the second time slot, the selected relay R_{n^*} forwards the signal to the users through DF protocol and superposition

[1]The type of satellite orbit is geosynchronous earth orbit (GEO), which has been used in several prior works [5], [6]. The delay for the GEO is a little larger, however, the advantages of the GEO can fill this shortage for its wide coverage, high reliability, etc.

[2]The two-user situation based on NOMA is assumed in our paper for the simplification in the analysis of the system performance and has been recognized by the Third Generation Partnership Project (3GPP) [33], [46], which is the basis of our future research with multi-user scenario.

[3]The single antenna is assumed for both the satellite and terrestrial devices to balance the system complexity, cost and system performance [20], which will be extended to multi-antenna situations in our future work.

coding technique, and we can get the received signal at the end of terrestrial users as

$$y_{U_i} = h_{R_{n^*}U_i}\left(\sqrt{P_R a_p}x_p + \sqrt{P_R a_q}x_q\right) + w_{R_{n^*}U_i}, \quad (5)$$

where P_R represents the transmission power of the selected relay R_{n^*}, $w_{R_{n^*}U_i}$ is the AWGN between R_{n^*} and U_i modeled as $w_{R_{n^*}U_i} \sim \mathcal{CN}\left(0, \sigma^2_{R_{n^*}U_i}\right)$, $h_{R_{n^*}U_i}$ is the channel coefficient of the selected relay R_{n^*} to users under Rayleigh fading satisfying $h_{R_{n^*}U_p} < h_{R_{n^*}U_q}$, the expression of $h_{R_{n^*}U_i}$ is ordinary given by

$$h_{R_{n^*}U_i} = \mathcal{F}_{R_{n^*}U_i} g_{R_{n^*}U_i}, \quad (6)$$

where $g_{R_{n^*}U_i}$ is the Rayleigh fading channel complex coefficient, $\mathcal{F}_{R_{n^*}U_i}$ represents channel parameters, which can be written as

$$\mathcal{F}_{R_{n^*}U_i} = \frac{1}{2}\left(20\lg\lambda - 10\varpi\lg\mathcal{D}_{R_{n^*}U_i} - 20\lg 4\pi\right), \quad (7)$$

with λ being the carrier center wavelength, $\varpi \in [2, 4]$ being the terrestrial path loss factor, $\mathcal{D}_{R_{n^*}U_i}$ being the distance of selected relay and terrestrial users.

III. PRELIMINARY RESULTS

In this section, we obtain the end-to-end SINR of the system along with the optimal relay selection scheme. In addition, the statistical properties of the channels for both SR fading and Rayleigh fading are given.

A. END-TO-END SINR OF THE SYSTEM

1) THE SINR AT R

Due to the application of NOMA procedure, the SIC technology is used to assist the receivers to receive the target signals. At first, the signal x_p with higher power is decoded at R, and x_q is treated as interference directly. Therefore, the SINR of signal x_p is given by

$$\gamma_{SR_{np}} = \frac{a_p\gamma_{SR_n}}{a_q\gamma_{SR_n} + 1}, \quad (8)$$

where γ_{SR_n} represents the instantaneous SNR of the terrestrial relays, $\gamma_{SR_n} = |h_{SR_n}|^2 P_S \Big/ \sigma^2_{SR_n} = \bar{\gamma}_{SR_n}|g_{SR_n}|^2$, and $\bar{\gamma}_{SR_n}$ is the average SNR of the satellite to the terrestrial-relays links, $\bar{\gamma}_{SR_n} = \mathcal{F}^2_{SR_n} P_S \Big/ \sigma^2_{SR_n}$.

Then, the receiver obtains the information of x_p, which can be eliminated from the received signal through SIC technology. However, due to the limitation of receiver performance and some other practical reasons such as synchronization error, residual impairments and error propagation during transmission and detection, it is worth assuming that imperfect SIC occurs at R and the SINR of signal x_q is expressed as

$$\gamma_{SR_{nq}} = \frac{a_q\gamma_{SR_n}}{\xi a_p\gamma_{SR_n} + 1}, \quad (9)$$

where ξ represents the proportional coefficient of residual interference resulted from imperfect SIC and $\xi \in (0, 1)$ [42].

2) THE SINR AT U_i

Similarly, the end-to-end SINR at U_i is derived. At first, x_p is decoded at U_p by considering x_q as interference, the SINR of x_p at U_p can be expressed as

$$\gamma_p = \frac{a_p\gamma_{R_{n^*}U_p}}{a_q\gamma_{R_{n^*}U_p} + 1}, \quad (10)$$

where $\gamma_{R_{n^*}U_p}$ represents the instantaneous SNR of the user U_p, $\gamma_{R_{n^*}U_p} = |h_{R_{n^*}U_p}|^2 P_R \Big/ \sigma^2_{R_{n^*}U_p} = \bar{\gamma}_{R_{n^*}U_p}|g_{R_{n^*}U_p}|^2$, and $\bar{\gamma}_{R_{n^*}U_p}$ is the average SNR of the selected relay R_{n^*} to the U_p, $\bar{\gamma}_{R_{n^*}U_p} = \mathcal{F}^2_{R_{n^*}U_p} P_R/\sigma^2_{R_{n^*}U_p}$.

The mission of U_q is to obtain the target signal x_q, according to the SIC technology of NOMA scheme, the signal x_p is decoded at U_q firstly, the SINR of x_p at U_q can be written as

$$\gamma_{q-p} = \frac{a_p\gamma_{R_{n^*}U_q}}{a_q\gamma_{R_{n^*}U_q} + 1}, \quad (11)$$

where $\gamma_{R_{n^*}U_q} = \bar{\gamma}_{R_{n^*}U_q}|g_{R_{n^*}U_q}|^2$ with $\bar{\gamma}_{R_{n^*}U_q} = \mathcal{F}^2_{R_{n^*}U_q} P_R/\sigma^2_{R_{n^*}U_q}$.

In the same way, recalling imperfect SIC as well, x_p is imperfectly eliminated from the received signal at U_q, the SINR of x_q at U_q is expressed as

$$\gamma_q = \frac{a_q\gamma_{R_{n^*}U_q}}{\xi a_p\gamma_{R_{n^*}U_q} + 1}. \quad (12)$$

B. SCHEME FOR RELAY SELECTION

Considering the spectrum efficiency and QoS requirements, the optimal relay needs to be selected to assist the transmission. Due to the high complexity of obtaining the overall CSI of the system [22], [27], we assume that we can only get the CSI of satellite-terrestrial links. Hence, the partial relay selection (PRS) scheme is used to select the optimal relay, which can be formulated as

$$n^* = \arg\max_n \left\{\gamma_{SR_n}\right\}. \quad (13)$$

The PRS scheme selects the relay with the maximum SNR in the first time slot as the optimal relay to forward the signal. As a matter of fact, due to the fast fading of satellite link channels and large propagation delay, it is difficult to acquire the perfect CSI of the satellite links, which has been investigated in detail [49], [50]. However, the main objective of this paper is to focus on the OP and EC performance of the NOMA-based ISTNs with relay selection and imperfect SIC, the perfect CSI of the satellite-terrestrial links is assumed to be the benchmark for analyzing system performance.

C. STATISTICAL PROPERTY OF THE CHANNEL

Before analyzing the system performance, the statistical properties of the channels of S-R links and R-U links are given first.

1) SATELLITE-RELAY CHANNEL

The channel of S-R links undergos SR fading channel [48], on the basis of (2), the probability density function (PDF) of

the squared amplitude of g_{SR_n} is given by

$$f_{|g_{SR_n}|^2}(x) = \alpha_{SR_n} e^{-\beta_{SR_n} x} {}_1F_1\left(m_{SR_n}; 1; \delta_{SR_n} x\right), \quad (14)$$

where $\alpha_{SR_n} \triangleq \frac{\left(\frac{2b_{SR_n} m_{SR_n}}{2b_{SR_n} m_{SR_n} + \Omega_{SR_n}}\right)^{m_{SR_n}}}{2b_{SR_n}}$, $\beta_{SR_n} \triangleq \frac{1}{2b_{SR_n}}$, $\delta_{SR_n} \triangleq \frac{\Omega_{SR_n}}{2b_{SR_n}(2b_{SR_n} m_{SR_n} + \Omega_{SR_n})}$, $\Omega_{SR_n}, 2b_{SR_n}$ and m_{SR_n} represent the average power of the line-of-sight (LOS) component, the average power of the multi-path component and the fading severity parameter with $m_{SR_n} \in (0, \infty)$, respectively.

Considering m_{SR_n} being integer values [9], after some mathematical transformation [47], the PDF can be rewritten as

$$f_{|g_{SR_n}|^2}(x) = \alpha_{SR_n} \sum_{k=0}^{m_{SR_n}-1} \zeta(k) x^k e^{-(\beta_{SR_n} - \delta_{SR_n})x}, \quad (15)$$

where $\zeta(k) = (-1)^k \binom{1 - m_{SR_n}}{k} \delta_{SR_n}^k / (k!)^2$. Write PDF in the form of SNR γ_{SR} $\left(SR \in \left\{SR_{np}, SR_{nq}\right\}\right)$ as

$$f_{\gamma_{SR}}(x) = \alpha_{SR_n} \sum_{k=0}^{m_{SR_n}-1} \frac{\zeta(k)}{\bar{\gamma}_{SR_n}^{k+1}} x^k e^{-\Delta_{SR_n} x}, \quad (16)$$

where $\Delta_{SR_n} = \frac{\beta_{SR_n} - \delta_{SR_n}}{\bar{\gamma}_{SR_n}}$.

With the help of [42, Eqs. 3.351.2], the cumulative distribution function (CDF) of γ_{SR} can be derived as

$$F_{\gamma_{SR}}(x) = 1 - \alpha_{SR_n} \sum_{k=0}^{m_{SR_n}-1} \frac{\zeta(k)}{\bar{\gamma}_{SR_n}^{k+1}} \sum_{t=0}^{k} \frac{k! x^t e^{-\Delta_{SR_n} x}}{t! \Delta_{SR_n}{}^{(k+1-t)}}. \quad (17)$$

2) TERRESTRIAL-TERRESTRIAL CHANNEL

The channel of $R - U$ links undergos Rayleigh fading channel [51], the PDF and CDF of SNR γ_{RU} $(RU \in \{p, q-p, q\})$ are, respectively, given by

$$f_{\gamma_{RU}}(x) = \frac{1}{\bar{\gamma}_{RU}} e^{-\frac{x}{\bar{\gamma}_{RU}}}, \quad (18)$$

$$F_{\gamma_{RU}}(x) = 1 - e^{-\frac{x}{\bar{\gamma}_{RU}}}, \quad (19)$$

where $\bar{\gamma}_{RU}$ means the average channel gain of relay to terrestrial users.

IV. OUTAGE PROBABILITY AND ASYMPTOTIC ANALYSIS

In this section, closed-form expression of OP for the NOMA-based ISTNs networks with PRS scheme and imperfect SIC is derived. To get deeper insights, the asymptotic expression of OP is given.

A. OP

OP is an important factor to investigate the performance of transmission in wireless communication system. The OP of the system means that the output SINR γ_e falls below a target threshold γ_{th}, which is defined as

$$P_{\gamma_e}(\gamma_{th}) = \Pr(\gamma_e \le \gamma_{th}), \quad (20)$$

where $\gamma_e = min(\gamma_{SR}, \gamma_{RU})$. In this paper, the whole system adopts DF protocol, which consists of two independent parts, $S - R$ links and $R - U$ links.

The overall OP of the system indicates that each transmission node is failed to decode the signal, and the whole system will be interrupted. Hence, the overall OP can be expressed as

$$P_{out} = 1 - \bar{P}_{out} = 1 - \underbrace{\Pr\left(\gamma_{SR_{n^*p}} \ge \gamma_{th}, \gamma_{SR_{n^*q}} \ge \gamma_{th}\right)}_{O_1} \times \underbrace{\Pr\left(\gamma_p \ge \gamma_{th}, \gamma_q \ge \gamma_{th}, \gamma_{q-p} \ge \gamma_{th}\right)}_{O_2}, \quad (21)$$

where O_1 and O_2 denote the probability of relay and users decoding signal successfully, respectively.

By substituting (8) and (9) into O_1, we can get

$$O_1 = \Pr\left\{\gamma_{SR_{n^*}} \ge \Upsilon_{\max}\right\} = \bar{F}_{\gamma_{SR_{n^*}}}(\Upsilon_{\max}), \quad (22)$$

where $\bar{F}_{\gamma_{SR_{n^*}}}(\cdot) = 1 - F_{\gamma_{SR_{n^*}}}(\cdot)$, $\Upsilon_{\max} = \max\{\Upsilon_{11}, \Upsilon_{12}\}$, the expressions of Υ_{11} and Υ_{12} are given in the below

$$\Upsilon_{11} = \frac{\gamma_{th}}{a_p - a_q \gamma_{th}}, a_p > a_q \gamma_{th}, \quad (23)$$

$$\Upsilon_{12} = \frac{\gamma_{th}}{a_q - \xi a_p \gamma_{th}}, a_q > \xi a_p \gamma_{th}. \quad (24)$$

Theorem 1: The CDF $F_{\gamma_{SR_{n^*}}}$ for the PRS scheme is given by

$$F_{\gamma_{SR_{n^*}}}(y) = 1 - \sum_{n=1}^{K} \binom{K}{n} (-1)^{n-1} \times \alpha_{SR}^n \Xi_{SR}^n y^{\Lambda_{SR}} e^{-n\Delta_{SR} y}, \quad (25)$$

where the expression of Ξ_{SR}^n is given at the bottom of the page as (26) *and the expression of Λ_{SR} is given in the below*

$$\Lambda_{SR} = \sum_{i=0}^{m_{SR}-1} i \times n_i. \quad (27)$$

Proof: See Appendix A. □

Hence, by applying (25) into (22), we can get the expression

$$O_1 = \sum_{n=1}^{K} \binom{K}{n} (-1)^{n-1} \alpha_{SR}^n \Xi_{SR}^n (\Upsilon_{\max})^{\Lambda_{SR}} e^{-n\Delta_{SR}\Upsilon_{\max}}. \quad (28)$$

$$\Xi_{SR}^n = \sum_{n_0=0}^{n} \sum_{n_1=0}^{n-n_0} \cdots \sum_{n_{m_{SR}-2}=0}^{n-\sum_{i=1}^{m_{SR}-3} n_i} \sum_{n_{m_{SR}-1}=0}^{n-\sum_{i=1}^{m_{SR}-2} n_i} \varphi_0^{n_0} \varphi_1^{n_1} \cdots \varphi_{m_{SR}-2}^{n_{m_{SR}-2}} \varphi_{m_{SR}-1}^{n_{m_{SR}-1}} \binom{n}{n_0, n_1, \cdots, n_{m_{SR}-2}, n_{m_{SR}-1}}, \quad (26)$$

By utilizing the similar method, we substitute (10), (11) and (12) into O_2, the expression of O_2 can be obtained as

$$\begin{aligned} O_2 &= \Pr\left\{\gamma_{R_{n^*}U_p} \geq \Upsilon_{11}\right\} \times \Pr\left\{\gamma_{R_{n^*}U_q} \geq \Upsilon_{\max}\right\} \\ &= \bar{F}_{\gamma_{R_{n^*}U_p}}(\Upsilon_{11}) \times \bar{F}_{\gamma_{R_{n^*}U_q}}(\Upsilon_{\max}). \end{aligned} \tag{29}$$

Assuming the channels of terrestrial relay to users links are independent and identically distributed, i.i.d., we can get $\bar{F}_{\gamma_{R_{n^*}U_p}}(\cdot) = \bar{F}_{\gamma_{R_{n^*}U_q}}(\cdot) = 1 - F_{\gamma_{RU}}(\cdot)$.

By substituting (19) into (29), the expression of O_2 can be rewritten as

$$O_2 = e^{-\frac{\Upsilon_{11}}{\bar{\gamma}_{R_{n^*}U_p}} - \frac{\Upsilon_{\max}}{\bar{\gamma}_{R_{n^*}U_q}}}. \tag{30}$$

At last, by utilizing (28) and (30) into (21), the final closed-form expression of the OP is obtained as (31), shown at the bottom of the page.

B. ASYMPTOTIC OP

To get more insights into the effects on the OP for the considered ISTNs in the high SNR regime, the asymptotic analysis for the OP is investigated in the following. To this end, it is assumed that $\overline{\gamma}_j$ tends to be infinite, and the CDF of γ_j is, respectively, obtained as

$$F^{\infty}_{\gamma_{SR}}(x) \approx \frac{\alpha_{SR}}{\bar{\gamma}_{SR}} x + o(x), \tag{32}$$

$$F^{\infty}_{\gamma_{RU}}(x) \approx \frac{x}{\bar{\gamma}_{RU}} + o(x), \tag{33}$$

where $o(x)$ means the higher order infinitesimal of x.

Applying the order statistics, the CDF of $\gamma_{SR_{n^*}}$ and γ_{RU} can be asymptotically denoted as

$$F^{\infty}_{\gamma_{SR_{n^*}}}(x) \overset{\Delta}{\simeq} \left(\frac{\alpha_{SR}}{\bar{\gamma}_{SR}} x\right)^K, \tag{34}$$

$$F^{\infty}_{\gamma_{RU}}(x) \overset{\Delta}{\simeq} \frac{x}{\bar{\gamma}_{RU}}. \tag{35}$$

With the similar approach, applying the asymptotic CDF to the expression of OP, (28) and (30) are, respectively, rewritten as

$$O_1 = 1 - \left(\frac{\alpha_{SR}}{\bar{\gamma}_{SR}} \Upsilon_{\max}\right)^K, \tag{36a}$$

$$O_2 = 1 - \frac{\Upsilon_{11}\Upsilon_{\max}}{(\bar{\gamma}_{RU})^2}. \tag{36b}$$

Therefore, by substituting (36a) and (36b) into (21), the final asymptotic expression of overall OP for the considered ISTNs can be derived as

$$\begin{aligned} P^{\infty}_{out} = \left(\frac{\alpha_{SR}}{\bar{\gamma}_{SR}} \Upsilon_{\max}\right)^K + \frac{\Upsilon_{11}\Upsilon_{\max}}{(\bar{\gamma}_{RU})^2} - \left(\frac{\alpha_{SR}}{\bar{\gamma}_{SR}}\right)^K \\ \times \frac{1}{(\bar{\gamma}_{RU})^2} \Upsilon_{11} (\Upsilon_{\max})^{K+1}. \end{aligned} \tag{37}$$

V. ERGODIC CAPACITY ANALYSIS

EC is another important factor to analyze the performance of the considered ISTNs. The overall EC of the system means the time average of the upper bound of the capacity on the each fading channel [52]. In this paper, the method of Meijer-G functions is used to get the expression of system EC. Owing to the system contains two time slots, the EC of the considered networks is defined as

$$EC = \min\left[EC_{SR}, EC_{RU}\right], \tag{38}$$

where EC_{SR} and EC_{RU} denote the EC of the satellite-relay links and the relay-terrestrial users links, respectively.

Theorem 2: The final expression of EC_{SR} is given by (39)*, as shown at the bottom of the page.*

Proof: See Appendix B. □

In the second time slot, EC is expressed as the sum of average instantaneous mutual information of the end-to-end SINR at U_i, on the basis of (10), (11) and (12), the expression of EC_{RU} is expressed as

$$\begin{aligned} EC_{RU} = \frac{1}{2}\left\{E\left[\log_2\left(1+\gamma_p\right)\right] + E\left[\log_2\left(1+\gamma_{q-p}\right)\right]\right. \\ \left. + E\left[\log_2\left(1+\gamma_q\right)\right]\right\}. \end{aligned} \tag{40}$$

The detailed derivation of the expression EC_{RU} is consistent with EC_{SR}, utilizing the similar method of Appendix B, the final expression of EC_{RU} is obtained as (41), shown at the bottom of the next page.

Finally, by substituting the final expressions of EC_{SR} and EC_{RU} into (38), the overall EC of the considered ISTNs is obtained. To reduce the space of this article, the final expression is omitted here.

$$P_{out} = 1 - \sum_{n=1}^{K} \binom{K}{n} (-1)^{n-1} \alpha_{SR}^n \Xi_{SR}^n (\Upsilon_{\max})^{\Lambda_{SR}} e^{-n\Delta_{SR}\Upsilon_{\max} - \frac{\Upsilon_{11}}{\bar{\gamma}_{R_{n^*}U_p}} - \frac{\Upsilon_{\max}}{\bar{\gamma}_{R_{n^*}U_q}}}. \tag{31}$$

$$\begin{aligned} EC_{SR} = \frac{1}{2\ln 2} K \sum_{k=0}^{m_{SR}-1} \frac{\zeta(k)}{\bar{\gamma}_{SR}^{k+1}} \sum_{n=0}^{K-1} \binom{K-1}{n} (-1)^n \alpha_{SR}^{n+1} \Xi_{SR}^n [(n+1)\Delta_{SR}]^{-(k+\Lambda_{SR}+1)} \\ \times \left\{ G_{23}^{31}\left((n+1)\Delta_{SR} \middle| \begin{matrix} 0,1 \\ k+\Lambda_{SR}+1,0,0 \end{matrix}\right) - G_{23}^{31}\left(\frac{(n+1)\Delta_{SR}}{a_q} \middle| \begin{matrix} 0,1 \\ k+\Lambda_{SR}+1,0,0 \end{matrix}\right) \right. \\ \left. + G_{23}^{31}\left(\frac{(n+1)\Delta_{SR}}{a_q+\xi a_p} \middle| \begin{matrix} 0,1 \\ 1+k,0,0 \end{matrix}\right) - G_{23}^{31}\left(\frac{(n+1)\Delta_{SR}}{\xi a_p} \middle| \begin{matrix} 0,1 \\ 1+k,0,0 \end{matrix}\right) \right\}. \end{aligned} \tag{39}$$

TABLE 1. System parameters.

Parameter	value
Satellite Orbit	GEO
Carrier Frequency	f=2GHz
Carrier Bandwidth	B=15MHz
3dB angle	$\varphi_{3\mathrm{dB}} = 0.8^{\circ}$
Maximal Beam Gain	$\mathcal{G}_{max} = 48dB$
Receive Antenna Gain	$\mathcal{G}_{r,SU_i} = 4dB$
Noise Temperature	$T = 300^{\circ}$
Terrestrial Path Loss	$\varpi = 2.5$
Relay-Terrestrial Distance	$\mathcal{D}_{R_{n^*}U_i} = 500m$

TABLE 2. SR fading channel parameters.

Shadowing	m_j	b_j	Ω_j
Frequent heavy shadowing (FHS)	1	0.063	0.0007
Average shadowing (AS)	5	0.251	0.279
Infrequent light shadowing (ILS)	10	0.158	1.29

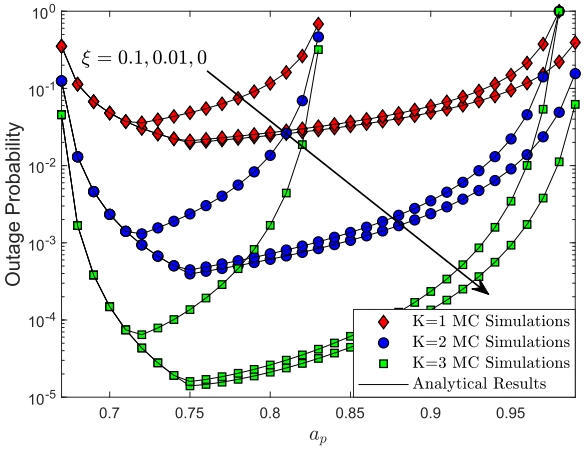

FIGURE 2. OP of the system versus different K and different ξ: FHS.

VI. NUMERICAL RESULTS

In this section, we investigate the key parameters on system performance of the considered ISTNs, and verify the analytical research under different conditions through MC simulations. For the simplification of the simulation, we suppose the AWGN and average SNR of the two time slots are identically, namely, $\sigma^2_{SR_n} = \sigma^2_{R_{n^*}U_i} = \sigma^2$ and $\bar{\gamma}_{SR_n} = \bar{\gamma}_{R_{n^*}U_i} = \overline{\rho}$ [13]. The system simulation parameters are given in Table 1 [9]. The SR fading channel parameters are given in Table 2 [21].

Fig. 2 illustrates the OP of the system versus a_p for different number of relays K and different imperfect SIC coefficient ξ for FHS scenario. Firstly, it can be easily observed from Fig. 2 that the MC simulations coincide with the analytical results, which verifies the correctness of our analytical derivation. Besides, the performance of OP outperforms with the increasing of the number of relays K, because the considered

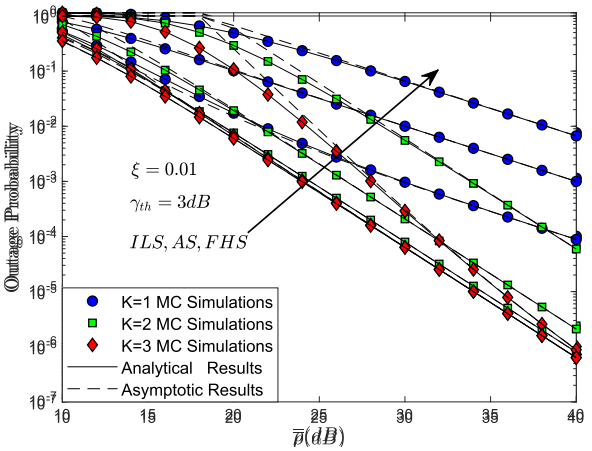

FIGURE 3. OP of the system versus different K and different channel parameters.

ISTNs can select the relay with the best channel from multiple relays for transmission. In addition, the OP degrades as the imperfection coefficient ξ increases, because when the receiver of U_q detects the signal x_q, it is interfered by the signal x_q under imperfect SIC. Moreover, the imperfect SIC coefficient will also influence the optimal power allocation coefficient, the larger the imperfect SIC coefficient ξ, the more complex the detection of signal x_q, and the more power will be allocated to the transmission of x_q.

Fig. 3. plots the OP of the system versus different number of relays K and different channel parameters. First of all, as the average SNR increases, the performance of the system OP will become better. Besides, the MC simulations are in line with the analytical results, meanwhile, the analytical analysis is in accordance with the trend of asymptotic analysis under a high SNR regime, which proves the accurateness and effectiveness of our analytical and asymptotic research. Moreover, the OP raises as channel conditions facilitate, which is consistent with common sense. However, when the number of relays K reaches 3, the OP will not continue to increase as the channel conditions get better under a high SNR regime. This is due to the reason that the OP of the considered ISTNs will not decrease indefinitely as the number of relays K increases. When K up to 3, OP will reach the lower bound.

Fig. 4. depicts the OP of the system versus $\overline{\rho}$ with different imperfect SIC coefficient ξ and different channel parameters. Clearly, MC simulations are in good agreement with theoretical analysis, as well as asymptotic results at high SNRs. Besides, the OP of the considered ISTNs decreases with the channel conditions deteriorating or experiencing worse imperfect SIC.

$$EC_{RU} = \frac{1}{2\ln 2}\left\{2G_{32}^{13}\left(\bar{\gamma}_{RU}\left|\begin{matrix}-1,1,1\\1,0\end{matrix}\right.\right) - 2G_{32}^{13}\left(a_q\bar{\gamma}_{RU}\left|\begin{matrix}-1,1,1\\1,0\end{matrix}\right.\right) + G_{32}^{13}\left(\left(a_q+\xi a_p\right)\bar{\gamma}_{RU}\left|\begin{matrix}-1,1,1\\1,0\end{matrix}\right.\right) - G_{32}^{13}\left(\xi a_p\bar{\gamma}_{RU}\left|\begin{matrix}-1,1,1\\1,0\end{matrix}\right.\right)\right\}. \quad (41)$$

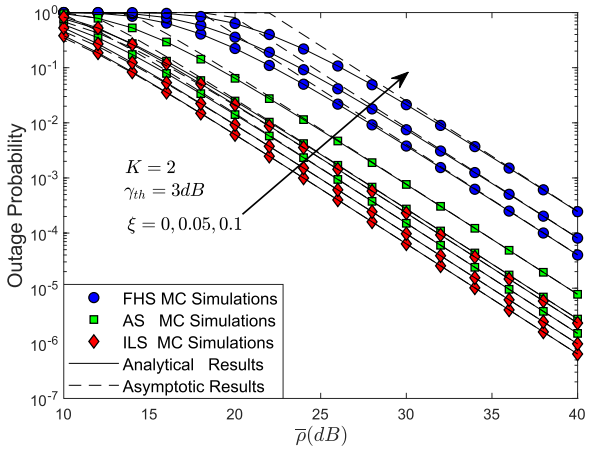

FIGURE 4. OP of the system versus different ξ and different channel parameters.

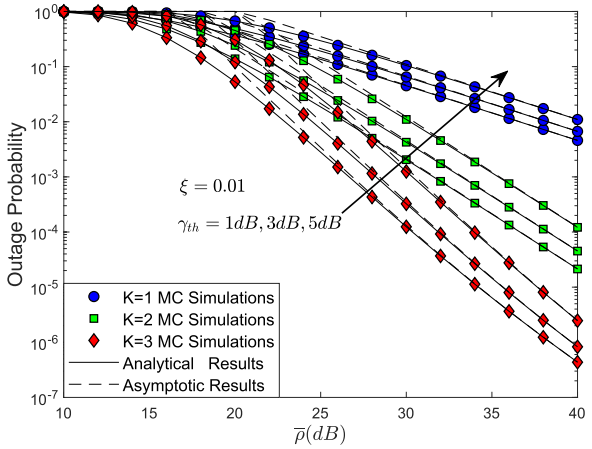

FIGURE 5. OP of the system versus different K and different γ_{th}: FHS.

Fig. 5. shows the OP of the system with different K and different outage threshold γ_{th}. It can be clearly observed that the OP becomes worse with the increasing of γ_{th} under the constraints of (23) and (24). Because when the outage threshold promotes, the overall system is more likely to be interrupted.

Fig. 6. illustrates the OP of the system versus $\overline{\rho}$ with different relay selection scheme and different K. It can be easily seen that the performance of the ORS scheme is better than that of the system with PRS scheme, which is similar with [27]. However, due to the complexity of CSI acquisition in the NOMA-based ISTRNs, there are only K links to obtain the CSI of satellite-terrestrial links for the PRS scheme, while 3K links are needed to obtain the overall CSI for the ORS scheme.

Fig. 7. depicts the EC of the system versus $\overline{\rho}$ with different K and different power coefficient a_p. Firstly, the MC simulations are consistent with analytical results, which verifies the correctness of our theoretical derivation of EC. Apparently, as the average SNR increases, the overall EC of the system will become more prominent and will gradually stabilize due to the limitation of the system transmission power under high

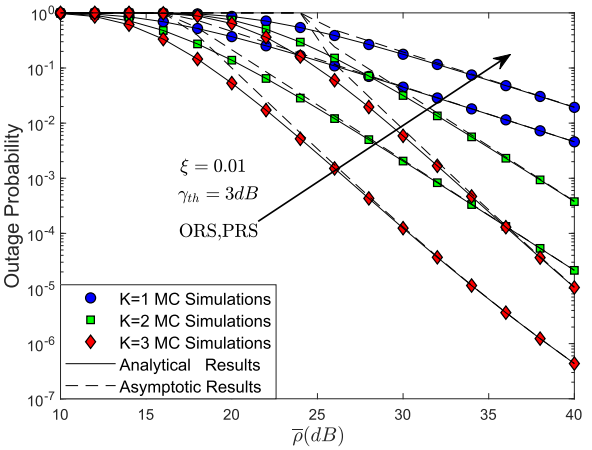

FIGURE 6. OP of the system versus different relay selection scheme and different K: FHS.

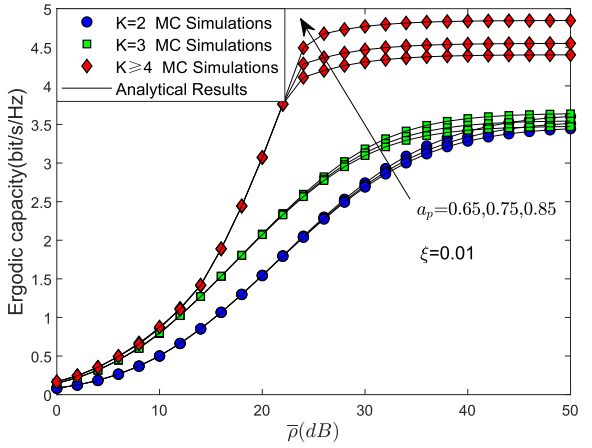

FIGURE 7. EC of the system versus different K and different a_p: FHS.

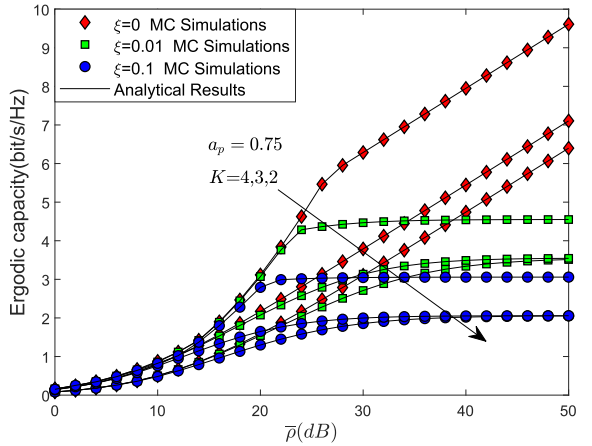

FIGURE 8. EC of the system versus different K and different ξ: FHS.

SNR. Besides, the overall EC depends on the smaller of the two time slots. When K is less than 4, the system EC is determined by the satellite-terrestrial link. When K exceeds 4, the system EC is determined by the relay-user link and will not increase with the increase of the relay numbers. Moreover, the EC improves with the rise of the power coefficient a_p.

Fig. 8. examines that EC of the system for different K and different ξ. Obviously, EC drops sharply as the increase of ξ in high SNR region, which indicates that the performance of EC is closely related to the imperfect SIC.

VII. CONCLUSION

In this paper, we analyzed the performance of NOMA-based ISTNs with the partial relay selection scheme and imperfect SIC. Based on the considered system model, the closed-form and asymptotic expressions of OP for the system were derived. Besides, the analysis for the EC is also derived. Simulation results denoted the performance of OP would be deteriorated as the condition of channels got worse or the system suffered imperfect SIC, and the performance of EC was sensitive to the imperfect SIC. Simultaneously, imperfect SIC resulted in the diversification of the optimal power allocation scheme. Furthermore, as the number of relays increased, the performance of OP and EC would upgrade and achieve the upper bound.

The NOMA-based ISTNs is a hot research topic, and we will expand our research on more benchmark problems in this field in our future work. In addition to OP and EC performance, delay is also an important indicator in the SatCom networks, and the performance analysis of system delay under satellites with different orbit could be adopted to satisfy the delay requirements of 5G and B5G networks [34], [46]. Moreover, the optimal power allocation scheme is another critical research hotspot [30], which can best improve the spectrum efficiency and meet the QoS requirements of different users.

APPENDIX A
PROOF OF THEOREM 1

According to the definition of PRS scheme and applying the order statistics [27], based on the assumption of the channels of satellite to relay links are independent and identically distributed, i.i.d., the CDF $F_{\gamma_{SR_{n^*}}}(y)$ of the system is given by

$$F_{\gamma_{SR_{n^*}}}(y) = \left[F_{\gamma_{SR}}(y)\right]^K. \tag{42}$$

By substituting (17) into (42), the $F_{\gamma_{SR_{n^*}}}(y)$ can be expressed as

$$F_{\gamma_{SR_{n^*}}}(y) = 1 - \sum_{n=1}^{K}\binom{K}{n}(-1)^{n-1}\left(\alpha_{SR}e^{-\Delta_{SR}y}\right)^n \times \underbrace{\left[\sum_{k=0}^{m_{SR}-1}\sum_{t=0}^{k}\frac{(-1)^k(1-m_{SR})_k\delta_{SR}^k}{k!\rho_1^{k+1}t!\Delta_{SR}^{(k+1-t)}}y^t\right]^n}_{\Phi(y)}. \tag{43}$$

After perform algebraic manipulation as $\sum_{k=0}^{l}\sum_{t=0}^{k}b_kc_ty^t = \sum_{t=0}^{l}\sum_{k=t}^{l}b_kc_ty^t$, $\Phi(y)$ can be rewritten as

$$\begin{aligned}\Phi(y) &= \left[\sum_{t=0}^{m_{SR}-1}\sum_{k=t}^{m_{SR}-1}\frac{(-1)^k(1-m_{SR})_k\delta_{SR}^k}{k!\rho_1^{k+1}t!\Delta_{SR}^{(k+1-t)}}y^t\right]^n \\ &= \left[\sum_{t=0}^{m_{SR}-1}\varphi_ty^t\right]^n,\end{aligned} \tag{44}$$

where $\varphi_t = \sum_{k=t}^{m_{SR}-1}\frac{(-1)^k(1-m_{SR})_k\delta_{SR}^k}{k!\rho_1^{k+1}t!\Delta_{SR}^{(k+1-t)}}$.

According to multinomial expansion identity theorem [54], we can re-express $\Phi(y)$ as

$$\Phi(y) = \sum_{n_i\geq 0, n_0+n_1+\cdots n_{m_{SR}-1}=n}\binom{n}{n_0, n_1, \cdots, n_{m_{SR}-1}} \times \prod_{0\leq i\leq m_{SR}-1}\left(\varphi_iy^i\right)^{n_i} \tag{45}$$

where $n_0, n_1, \cdots, n_{m_{SR}-1}$ are non-negative integers satisfying $n_0 + n_1 + \cdots + n_{m_{SR}-2} + n_{m_{SR}-1} = n$, and $\binom{n}{n_0, n_1, \cdots, n_{m_{SR}-1}} = \frac{n!}{n_0!n_1!\cdots n_{m_{SR}-1}!}$.

Now, substituting (45) into (43) and after simple sorting, the final expression of $F_{\gamma_{SR_{n^*}}}(y)$ can be written as (25) in Theorem 1.

APPENDIX B
PROOF OF THEOREM 2

In the first time slot, EC is expressed as the sum of the mean of the instantaneous mutual information of the end-to-end SINR at R [17], [52], with the help of (8) and (9), EC_{SR} is defined as

$$EC_{SR} = \frac{1}{2}\left\{E\left[\log_2\left(1+\gamma_{SR_{n^*p}}\right)\right] + E\left[\log_2\left(1+\gamma_{SR_{n^*q}}\right)\right]\right\}, \tag{46}$$

where the coefficient 1/2 is needed here as a result of DF protocol.

After some manipulation steps, EC_{SR} can be obtained as

$$\begin{aligned}EC_{SR} &= \frac{1}{2\ln 2}\left\{E\left[\ln\left(\gamma_{SR_{n^*}}+1\right)\right] - E\left[\ln\left(a_q\gamma_{SR_{n^*}}+1\right)\right]\right. \\ &\quad + E\left[\ln\left(\left(a_q+\xi a_p\right)\gamma_{SR_{n^*}}+1\right)\right] \\ &\quad \left. - E\left[\ln\left(\xi a_p\gamma_{SR_{n^*}}+1\right)\right]\right\}.\end{aligned} \tag{47}$$

Let $\gamma_{SR_{n^*}} = x$, $a_q\gamma_{SR_{n^*}} = z_1$, $\left(a_q+\xi a_p\right)\gamma_{SR_{n^*}} = z_2$, and $\xi a_p\gamma_{SR_{n^*}} = z_3$, with the help of probability transformation formula, the PDFs of z_1, z_2, z_3 can be respectively calculated as

$$f_{z_1}(z) = \frac{1}{a_q}f_x\left(\frac{1}{a_q}z\right), \tag{48a}$$

$$f_x(z) = K\sum_{k=0}^{m_{SR}-1}\frac{\zeta(k)}{\bar{\gamma}_{SR}^{k+1}}\sum_{n=0}^{K-1}\binom{K-1}{n}(-1)^n\alpha_{SR}^{n+1}\Xi_{SR}^n z^{k+\Lambda_{SR}}e^{-(n+1)\Delta_{SR}z}. \tag{50}$$

$$f_{z_1}(z) = K\sum_{k=0}^{m_{SR}-1}\frac{\zeta(k)}{\bar{\gamma}_{SR}^{k+1}}\sum_{n=0}^{K-1}\binom{K-1}{n}(-1)^n\alpha_{SR}^{n+1}\Xi_{SR}^n\left(\frac{1}{a_q}\right)^{k+\Lambda_{SR}+1} z^{k+\Lambda_{SR}}e^{-\frac{(n+1)\Delta_{SR}}{a_q}z}. \tag{51}$$

$$f_{z_2}(z) = K\sum_{k=0}^{m_{SR}-1}\frac{\zeta(k)}{\bar{\gamma}_{SR}^{k+1}}\sum_{n=0}^{K-1}\binom{K-1}{n}(-1)^n\alpha_{SR}^{n+1}\Xi_{SR}^n\left(\frac{1}{a_q+\xi a_p}\right)^{k+\Lambda_{SR}+1} z^{k+\Lambda_{SR}}e^{-\frac{(n+1)\Delta_{SR}}{a_q+\xi a_p}z}. \tag{52}$$

$$f_{z_3}(z) = K\sum_{k=0}^{m_{SR}-1}\frac{\zeta(k)}{\bar{\gamma}_{SR}^{k+1}}\sum_{n=0}^{K-1}\binom{K-1}{n}(-1)^n\alpha_{SR}^{n+1}\Xi_{SR}^n\left(\frac{1}{\xi a_p}\right)^{k+\Lambda_{SR}+1} z^{k+\Lambda_{SR}}e^{-\frac{(n+1)\Delta_{SR}}{\xi a_p}z}. \tag{53}$$

$$Q_1 = K\sum_{k=0}^{m_{SR}-1}\frac{\zeta(k)}{\bar{\gamma}_{SR}^{k+1}}\sum_{n=0}^{K-1}\binom{K-1}{n}(-1)^n\alpha_{SR}^{n+1}\Xi_{SR}^n[(n+1)\Delta_{SR}]^{-(k+\Lambda_{SR}+1)}G_{23}^{31}\left((n+1)\Delta_{SR}\middle|\begin{matrix}0,1\\k+\Lambda_{SR}+1,00\end{matrix}\right). \tag{56}$$

$$Q_2 = K\sum_{k=0}^{m_{SR}-1}\frac{\zeta(k)}{\bar{\gamma}_{SR}^{k+1}}\sum_{n=0}^{K-1}\binom{K-1}{n}(-1)^n\alpha_{SR}^{n+1}\Xi_{SR}^n[(n+1)\Delta_{SR}]^{-(k+\Lambda_{SR}+1)}G_{23}^{31}\left(\frac{(n+1)\Delta_{SR}}{a_q}\middle|\begin{matrix}0,1\\k+\Lambda_{SR}+1,00\end{matrix}\right). \tag{57}$$

$$Q_3 = K\sum_{k=0}^{m_{SR}-1}\frac{\zeta(k)}{\bar{\gamma}_{SR}^{k+1}}\sum_{n=0}^{K-1}\binom{K-1}{n}(-1)^n\alpha_{SR}^{n+1}\Xi_{SR}^n[(n+1)\Delta_{SR}]^{-(k+\Lambda_{SR}+1)}G_{23}^{31}\left(\frac{(n+1)\Delta_{SR}}{a_q}\middle|\begin{matrix}0,1\\k+\Lambda_{SR}+1,00\end{matrix}\right). \tag{58}$$

$$Q_4 = K\sum_{k=0}^{m_{SR}-1}\frac{\zeta(k)}{\bar{\gamma}_{SR}^{k+1}}\sum_{n=0}^{K-1}\binom{K-1}{n}(-1)^n\alpha_{SR}^{n+1}\Xi_{SR}^n[(n+1)\Delta_{SR}]^{-(k+\Lambda_{SR}+1)}G_{23}^{31}\left(\frac{(n+1)\Delta_{SR}}{a_q}\middle|\begin{matrix}0,1\\k+\Lambda_{SR}+1,00\end{matrix}\right). \tag{59}$$

$$f_{z_2}(z) = \frac{1}{a_q+\xi a_p}f_x\left(\frac{1}{a_q+\xi a_p}z\right), \tag{48b}$$

$$f_{z_3}(z) = \frac{1}{\xi a_p}f_x\left(\frac{1}{\xi a_p}z\right). \tag{48c}$$

Applying the order statistics, the PDF of $\gamma_{SR_{n^*}}$ can be derived as

$$f_x(z) = f_{\gamma_{SR_{n^*}}}(z) = Kf_{\gamma_{SR_n}}(z)F_{\gamma_{SR_n}}^{K-1}(z). \tag{49}$$

By substituting (16) and (17) into (49), referring to Appendix A, $f_x(z)$ is obtained as (50) at the top of the page.

Therefore, by applying (50) into (48a), (48b) and (48c), the corresponding PDF expressions can be equally obtained as (51), (52) and (53), shown at the top of the page.

Then, the expression of EC_{SR} can be rewritten as

$$EC_{SR} = \frac{1}{2\ln 2}\times\left\{\underbrace{\int_0^\infty \ln(z+1)f_x(z)\,dz}_{Q_1} - \underbrace{\int_0^\infty \ln(z+1)f_{z_1}(z)\,dz}_{Q_2} + \underbrace{\int_0^\infty \ln(z+1)f_{z_2}(z)\,dz}_{Q_3} - \underbrace{\int_0^\infty \ln(z+1)f_{z_3}(z)\,dz}_{Q_4}\right\}. \tag{54}$$

With the help of [46, Eq.8.4.6.5], Meijer-G function [42, Eq. 9.301] is used to analysis EC, namely,

$$\ln(1+z) = G_{22}^{12}\left(z\middle|\begin{matrix}1,\ 1\\1\ \ 0\end{matrix}\right). \tag{55}$$

By substituting (55) into Q_1, with the help of [46, Eq.2.24.3.1] and [46, Eq.8.2.2.14], Q_1 can be expressed as (56) at the top of the page.

Applying the similar way, we can also get the expressions of Q_2, Q_3 and Q_4, respectively.

At last, by substituting the expressions of Q_1, Q_2, Q_3 and Q_4 into (54), the final expression of EC_{SR} can be obtained as (39) in Theorem 2.

REFERENCES

[1] D. Tse and P. Viswanath, *Fundamentals of Wireless Communication*. Cambridge, U.K.: Cambridge Univ. Press, 2005.

[2] K. Y. Jo, *Satellite Communications Netwowrk Design and Analysis*. Norwood, MA, USA: Artech House, 2011.

[3] Z. Lin, M. Lin, T. de Cola, J.-B. Wang, W.-P. Zhu, and J. Cheng, "Supporting IoT with rate-splitting multiple access in satellite and aerial-integrated networks," *IEEE Internet Things J.*, vol. 8, no. 14, pp. 11123–11134, Jul. 2021.

[4] Q. Huang, M. Lin, W.-P. Zhu, J. Cheng, and M.-S. Alouini, "Uplink massive access in mixed RF/FSO satellite-aerial-terrestrial networks," *IEEE Trans. Commun.*, vol. 69, no. 4, pp. 2413–2426, Apr. 2021.

[5] K. Guo, K. An, B. Zhang, Y. Huang, X. Tang, G. Zheng, and T. A. Tsiftsis, "Physical layer security for multiuser satellite communication systems with threshold-based scheduling scheme," *IEEE Trans. Veh. Technol.*, vol. 69, no. 5, pp. 5129–5141, May 2020.

[6] Z. Lin, M. Lin, J. Ouyang, W.-P. Zhu, A. D. Panagopoulos, and M.-S. Alouini, "Robust secure beamforming for multibeam satellite communication systems," *IEEE Trans. Veh. Technol.*, vol. 68, no. 6, pp. 6202–6206, Jun. 2019.

[7] Z. Lin, M. Lin, B. Champagne, W.-P. Zhu, and N. Al-Dhahir, "Secure and energy efficient transmission for RSMA-based cognitive satellite-terrestrial networks," *IEEE Wireless Commun. Lett.*, vol. 10, no. 2, pp. 251–255, Feb. 2021.
[8] K. An and T. Liang, "Hybrid satellite-terrestrial relay networks with adaptive transmission," *IEEE Trans. Veh. Technol.*, vol. 68, no. 12, pp. 12448–12452, Dec. 2019.
[9] K. Guo, M. Lin, B. Zhang, W.-P. Zhu, J.-B. Wang, and T. A. Tsiftsis, "On the performance of LMS communication with hardware impairments and interference," *IEEE Trans. Commun.*, vol. 67, no. 2, pp. 1490–1505, Feb. 2019.
[10] K. Guo, K. An, B. Zhang, Y. Huang, and G. Zheng, "Outage analysis of cognitive hybrid satellite-terrestrial networks with hardware impairments and multi-primary users," *IEEE Wireless Commun. Lett.*, vol. 7, no. 5, pp. 816–819, Oct. 2018.
[11] K. An, M. Lin, T. Liang, J.-B. Wang, J. Wang, Y. Huang, and A. L. Swindlehurst, "Performance analysis of multi-antenna hybrid satellite-terrestrial relay networks in the presence of interference," *IEEE Trans. Commun.*, vol. 63, no. 11, pp. 4390–4404, Nov. 2015.
[12] M. Lin, Q. Huang, T. de Cola, J.-B. Wang, J. Wang, M. Guizani, and J.-Y. Wang, "Integrated 5G-satellite networks: A perspective on physical layer reliability and security," *IEEE Wireless Commun.*, vol. 27, no. 6, pp. 152–159, Dec. 2020.
[13] K. Guo, K. An, F. Zhou, T. A. Tsiftsis, G. Zheng, and S. Chatzinotas, "On the secrecy performance of NOMA-based integrated satellite multiple-terrestrial relay networks with hardware impairments," *IEEE Trans. Veh. Technol.*, vol. 70, no. 4, pp. 3661–3676, Apr. 2021.
[14] Z. Ding, X. Lei, G. K. Karagiannidis, R. Schober, J. Yuan, and V. Bhargava, "A survey on non-orthogonal multiple access for 5G networks: Research challenges and future trends," *IEEE J. Sel. Areas Commun.*, vol. 35, no. 10, pp. 2181–2195, Oct. 2017.
[15] Y. Liu, Z. Qin, M. Elkashlan, Z. Ding, A. Nallanathan, and L. Hanzo, "Nonorthogonal multiple access for 5G and beyond," *Proc. IEEE*, vol. 105, no. 12, pp. 2347–2381, Dec. 2017.
[16] V. Singh, P. K. Upadhyay, and M. Lin, "On the performance of NOMA-assisted overlay multiuser cognitive satellite-terrestrial networks," *IEEE Wireless Commun. Lett.*, vol. 9, no. 5, pp. 638–642, May 2020.
[17] Q. Huang, M. Lin, W.-P. Zhu, S. Chatzinotas, and M.-S. Alouini, "Performance analysis of integrated satellite-terrestrial multiantenna relay networks with multiuser scheduling," *IEEE Trans. Aerosp. Electron. Syst.*, vol. 56, no. 4, pp. 2718–2731, Aug. 2020.
[18] K. An *et al.*, "Outage performance of cognitive hybrid satellite-terrestrial networks with interference constraint," *IEEE Trans. Veh. Technol.*, vol. 65, no. 11, pp. 9397–9404, Nov. 2016.
[19] Q. Huang, M. Lin, J. Wang, T. A. Tsiftsis, and J. Wang, "Energy efficient beamforming schemes for satellite-aerial-terrestrial networks," *IEEE Trans. Commun.*, vol. 68, no. 6, pp. 3863–3875, Jun. 2020.
[20] R. Liu, K. Guo, K. An, S. Zhu, and H. Shuai, "NOMA-based integrated satellite-terrestrial relay networks under spectrum sharing environment," *IEEE Wireless Commun. Lett.*, vol. 10, no. 6, pp. 1266–1270, Jun. 2021.
[21] K. Guo, K. An, B. Zhang, Y. Huang, D. Guo, G. Zheng, and S. Chatzinotas, "On the performance of the uplink satellite multiterrestrial relay networks with hardware impairments and interference," *IEEE Syst. J.*, vol. 13, no. 3, pp. 2297–2308, Sep. 2019.
[22] K. Guo, M. Lin, B. Zhang, J.-B. Wang, Y. Wu, W.-P. Zhu, and J. Cheng, "Performance analysis of hybrid satellite-terrestrial cooperative networks with relay selection," *IEEE Trans. Veh. Technol.*, vol. 69, no. 8, pp. 9053–9067, Aug. 2020.
[23] Z. Ding, H. Dai, and H. V. Poor, "Relay selection for cooperative NOMA," *IEEE Wireless Commun. Lett.*, vol. 5, no. 4, pp. 416–419, Aug. 2016.
[24] Z. Yang, Z. Ding, Y. Wu, and P. Fan, "Novel relay selection strategies for cooperative NOMA," *IEEE Trans. Veh. Technol.*, vol. 66, no. 11, pp. 10114–10123, Nov. 2017.
[25] X. Yue, Y. Liu, S. Kang, A. Nallanathan, and Z. Ding, "Spatially random relay selection for full/half-duplex cooperative NOMA networks," *IEEE Trans. Commun.*, vol. 66, no. 8, pp. 3294–3308, Aug. 2018.
[26] P. K. Upadhyay and P. K. Sharma, "Max-max user-relay selection scheme in multiuser and multirelay hybrid satellite-terrestrial relay systems," *IEEE Commun. Lett.*, vol. 20, no. 2, pp. 268–271, Feb. 2016.
[27] P. K. Sharma, P. K. Upadhyay, D. B. da Costa, P. S. Bithas, and A. G. Kanatas, "Performance analysis of overlay spectrum sharing in hybrid satellite-terrestrial systems with secondary network selection," *IEEE Trans. Wireless Commun.*, vol. 16, no. 10, pp. 6586–6601, Oct. 2017.
[28] K. An, Y. Li, X. Yan, and T. Liang, "On the performance of cache-enabled hybrid satellite-terrestrial relay networks," *IEEE Wireless Commun. Lett.*, vol. 8, no. 5, pp. 1506–1509, Oct. 2019.
[29] X. Zhang, K. An, B. Zhang, Z. Chen, Y. Yan, and D. Guo, "Vickrey auction-based secondary relay selection in cognitive hybrid satellite-terrestrial overlay networks with non-orthogonal multiple access," *IEEE Wireless Commun. Lett.*, vol. 9, no. 5, pp. 628–632, May 2020.
[30] M. Vaezi, R. Schober, Z. Ding, and H. V. Poor, "Non-orthogonal multiple access: Common myths and critical questions," *IEEE Wireless Commun.*, vol. 26, no. 5, pp. 174–180, Oct. 2019.
[31] X. Yan, H. Xiao, K. An, and C.-X. Wang, "Outage performance of NOMA-based hybrid satellite-terrestrial relay networks," *IEEE Wireless Commun. Lett.*, vol. 7, no. 4, pp. 538–541, Aug. 2018.
[32] X. Yan, H. Xiao, K. An, G. Zheng, and W. Tao, "Hybrid satellite terrestrial relay networks with cooperative non-orthogonal multiple access," *IEEE Commun. Lett.*, vol. 22, no. 5, pp. 978–981, May 2018.
[33] X. Yan, H. Xiao, K. An, G. Zheng, and S. Chatzinotas, "Ergodic capacity of NOMA-based uplink satellite networks with randomly deployed users," *IEEE Syst. J.*, vol. 14, no. 3, pp. 3343–3350, Sep. 2020.
[34] M. Karavolos, N. Nomikos, and D. Vouyioukas, "Enhanced integrated satellite-terrestrial NOMA with cooperative device-to-device communication," *Telecom*, vol. 1, no. 2, pp. 126–149, Sep. 2020.
[35] L. Han, W.-P. Zhu, and M. Lin, "Outage of NOMA-based hybrid satellite-terrestrial multi-antenna DF relay networks," *IEEE Wireless Commun. Lett.*, vol. 10, no. 5, pp. 1083–1087, May 2021.
[36] X. Zhang, B. Zhang, K. An, B. Zhao, Y. Jia, Z. Chen, and D. Guo, "On the performance of hybrid satellite-terrestrial content delivery networks with non-orthogonal multiple access," *IEEE Wireless Commun. Lett.*, vol. 10, no. 3, pp. 454–458, Mar. 2021.
[37] Z. Lin, M. Lin, J.-B. Wang, T. de Cola, and J. Wang, "Joint beamforming and power allocation for satellite-terrestrial integrated networks with non-orthogonal multiple access," *IEEE J. Sel. Areas Commun.*, vol. 13, no. 3, pp. 657–670, Jun. 2019.
[38] W. Lu, K. An, T. Liang, and X. Yan, "Robust beamforming in multibeam satellite systems with non-orthogonal multiple access," *IEEE Wireless Commun. Lett.*, vol. 9, no. 11, pp. 1889–1893, Nov. 2020.
[39] Z. Ding, R. Schober, and H. V. Poor, "Unveiling the importance of SIC in NOMA systems—Part 1: State of the art and recent findings," *IEEE Commun. Lett.*, vol. 24, no. 11, pp. 2373–2377, Nov. 2020.
[40] Z. Ding, R. Schober, and H. V. Poor, "Unveiling the importance of SIC in NOMA systems—Part II: New results and future directions," *IEEE Commun. Lett.*, vol. 24, no. 11, pp. 2378–2382, Nov. 2020.
[41] F. Kara and H. Kaya, "Improved user fairness in decode-forward relaying non-orthogonal multiple access schemes with imperfect SIC and CSI," *IEEE Access*, vol. 8, pp. 97540–97556, 2020.
[42] X. Li, M. Liu, C. Deng, P. T. Mathiopoulos, Z. Ding, and Y. Liu, "Full-duplex cooperative NOMA relaying systems with I/Q imbalance and imperfect SIC," *IEEE Wireless Commun. Lett.*, vol. 9, no. 1, pp. 17–20, Jan. 2020.
[43] X. Li, M. Zhao, M. Zeng, S. Mumtaz, V. G. Menon, Z. Ding, and O. A. Dobre, "Hardware impaired ambient backscatter NOMA systems: Reliability and security," *IEEE Trans. Commun.*, vol. 69, no. 4, pp. 2723–2736, Apr. 2021.
[44] L. Han, W.-P. Zhu, and M. Lin, "Outage analysis of NOMA-based multiple-antenna hybrid satellite-terrestrial relay networks," *IEEE Commun. Lett.*, vol. 25, no. 4, pp. 1109–1113, Apr. 2021.
[45] X. Yue, Y. Liu, Y. Yao, T. Li, X. Li, R. Liu, and A. Nallanathan, "Outage behaviors of NOMA-based satellite network over shadowed-Rician fading channels," *IEEE Trans. Veh. Technol.*, vol. 69, no. 6, pp. 6818–6821, Jun. 2020.
[46] J. Zhao, X. Yue, S. Kang, and W. Tang, "Joint effects of imperfect CSI and SIC on NOMA based satellite-terrestrial systems," *IEEE Access*, vol. 9, pp. 12545–12554, 2021.
[47] I. S. Gradshteyn and I. M. Ryzhik, *Table of Integrals, Series and Products*, 7th ed. Amsterdam, The Netherlands: Elsevier, 2007.
[48] A. Abdi, W. C. Lau, M.-S. Alouini, and M. Kaveh, "A new simple model for land mobile satellite channels: First- and second-order statistics," *IEEE Trans. Wireless Commun*, vol. 2, no. 3, pp. 519–528, May 2003.
[49] M. K. Arti, "Channel estimation and detection in satellite communication systems," *IEEE Trans. Veh. Technol.*, vol. 65, no. 12, pp. 10173–10179, Dec. 2016.
[50] M. K. Arti, "Channel estimation and detection in hybrid satellite-terrestrial communication systems," *IEEE Trans. Veh. Technol.*, vol. 65, no. 7, pp. 5764–5771, Jul. 2016.

[51] A. Bletsas, H. Shin, and M. Win, "Cooperative communications with outage-optimal opportunistic relaying," *IEEE Trans. Wireless Commun.*, vol. 6, no. 9, pp. 3450–3460, Sep. 2007.
[52] G. Farhadi and N. C. Beaulieu, "On the ergodic capacity of multi-hop wireless relaying systems," *IEEE Trans. Wireless Commun.*, vol. 8, no. 5, pp. 2286–2291, May 2009.
[53] A. P. Prudnikov, Y. A. Brychkov, and O. I. Marichev, *Integrals and Series: More Special Functions*, vol. 3. New York, NY, USA: Gordon and Breach, 1990.
[54] R. L. Graham, D. E. Knuth, and O. Patashnik, *Concrete Mathematics*. New York, NY, USA: Addison-Wesley, 1989.

HAIFENG SHUAI received the B.S. degree from Tianjin University of Science and Technology, Tianjin, China, in 2017, and the M.S. degree from Space Engineering University, Beijing, China, in 2019, where he is currently pursuing the Ph.D. degree. His research interests include satellite-terrestrial networks, non-orthogonal multiple access, wireless communication systems, and multiuser communication systems.

KEFENG GUO received the B.S. degree from Beijing Institute of Technology, Beijing, China, in 2012, the M.S. degree from PLA University of Science and Technology, Nanjing, China, in 2015, and the Ph.D. degree from Army Engineering University of PLA, in 2018.

He is currently a Lecturer with the School of Space Information, Space Engineering University. He has authored or coauthored nearly 50 research articles in international journals and conferences. His research interests include cooperative relay networks, MIMO communications systems, multiuser communication systems, satellite communication, hardware impairments, cognitive radio, NOMA technology, and physical layer security. He has been a TPC Member of many IEEE sponsored conferences, such as IEEE ICC, IEEE GLOBECOM, and IEEE WCNC.

KANG AN received the B.S. degree from Nanjing University of Aeronautics and Astronautics, Nanjing, China, in 2011, the M.S. degree from PLA University of Science and Technology, Nanjing, and the Ph.D. degree from Army Engineering University of PLA, in 2017. He is currently a Senior Engineer with the Sixty-Third Research Institute, National University of Defense Technology, Nanjing. His research interests include cooperative communication, satellite communication, cognitive radio, and physical layer security.

SHIBING ZHU received the B.S. degree from the Equipment College, Beijing, China, in 1992, the M.S. degree from National Defense University, Beijing, in 1997, and the Ph.D. degree from Wuhan University of Technology, Wuhan, China, in 2009. He is currently a Professor and a Doctoral Supervisor with Space Engineering University. His current research interests include spatial information network and security and 5G mobile communication.